


Characterizing the complexity of time series networks of dynamical systems: A simplicial approach

Cite as: Chaos **30**, 013109 (2020); <https://doi.org/10.1063/1.5100362>

Submitted: 17 April 2019 . Accepted: 09 December 2019 . Published Online: 07 January 2020

Malayaja Chutani , Nithyanand Rao, N. Nirmal Thyagu , and Neelima Gupte

COLLECTIONS

 This paper was selected as Featured



View Online



Export Citation



CrossMark

ARTICLES YOU MAY BE INTERESTED IN

[How entropic regression beats the outliers problem in nonlinear system identification](#)

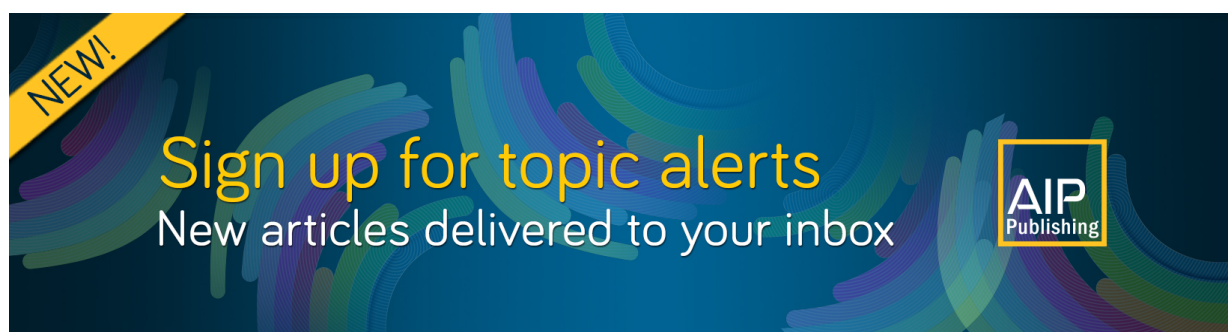
Chaos: An Interdisciplinary Journal of Nonlinear Science **30**, 013107 (2020); <https://doi.org/10.1063/1.5133386>

[Using machine learning to predict extreme events in the Hénon map](#)

Chaos: An Interdisciplinary Journal of Nonlinear Science **30**, 013113 (2020); <https://doi.org/10.1063/1.5121844>

[Reconstructing bifurcation diagrams only from time-series data generated by electronic circuits in discrete-time dynamical systems](#)

Chaos: An Interdisciplinary Journal of Nonlinear Science **30**, 013128 (2020); <https://doi.org/10.1063/1.5119187>



Characterizing the complexity of time series networks of dynamical systems: A simplicial approach

Cite as: Chaos 30, 013109 (2020); doi: 10.1063/1.5100362

Submitted: 17 April 2019 · Accepted: 9 December 2019 ·

Published Online: 7 January 2020



View Online



Export Citation



CrossMark

Malayaja Chutani,^{1,a)}  Nithyanand Rao,² N. Nirmal Thyagu,^{3,b)}  and Neelima Gupta^{1,c)}

AFFILIATIONS

¹Department of Physics, Indian Institute of Technology Madras, Chennai 600036, India

²Department of Mathematics, Indian Institute of Technology Madras, Chennai 600036, India

³Division of Physics, School of Advanced Sciences, Vellore Institute of Technology, Chennai 600127, India

^{a)}malayajac@physics.iitm.ac.in

^{b)}**Present address:** Department of Physics, Madras Christian College, Tambaram, Chennai 600059, India.

^{c)}gupte@physics.iitm.ac.in

ABSTRACT

We analyze the time series obtained from different dynamical regimes of evolving maps and flows by constructing their equivalent time series networks, using the visibility algorithm. The regimes analyzed include periodic, chaotic, and hyperchaotic regimes, as well as intermittent regimes and regimes at the edge of chaos. We use the methods of algebraic topology, in particular, simplicial complexes, to define simplicial characterizers, which can analyze the simplicial structure of the networks at both the global and local levels. The simplicial characterizers bring out the hierarchical levels of complexity at various topological levels. These hierarchical levels of complexity find the skeleton of the local dynamics embedded in the network, which influence the global dynamical properties of the system and also permit the identification of dominant motifs. We also analyze the same networks using conventional network characterizers such as average path lengths and clustering coefficients. We see that the simplicial characterizers are capable of distinguishing between different dynamical regimes and can pick up subtle differences in dynamical behavior, whereas the usual characterizers provide a coarser characterization. However, the two taken in conjunction can provide information about the dynamical behavior of the time series, as well as the correlations in the evolving system. Our methods can, therefore, provide powerful tools for the analysis of dynamical systems.

Published under license by AIP Publishing. <https://doi.org/10.1063/1.5100362>

We use the methods of algebraic topology, viz., the construction of simplicial characterizers to analyze the hidden geometry of time series (TS) networks. These TS networks are constructed using the visibility algorithm from time series corresponding to distinct dynamical regimes of a variety of dynamical systems, such as the logistic, Hénon, and generalized Lozi maps, and the Lorenz attractor. The TS networks are constructed using the visibility algorithm, and the dynamical regimes analyzed include periodic, intermittent, chaotic, and hyperchaotic behavior, as well as the Feigenbaum attractor, which typifies the regime at the edge of chaos. The TS network graphs are seen to contain the signature of each dynamical regime, as well as that of the short term correlations in the evolution of the system. The simplicial characterizers uncover the hidden geometry of these graphs, level by simplicial level, by providing a precise quantification of the manner

in which these graphs are connected, pointwise, linkwise, trianglewise, and higher. Our analysis shows that the simplicial characterizers are capable of distinguishing clearly between different dynamical regimes and can pick up subtle differences in dynamical behavior. A local simplicial quantity, the $\max(\dim)Q^i$, which is the number of simplices in which the most connected node participates, can serve as a single characterizer of the dynamical complexity of the time series and shows clearly differentiated values for periodic, chaotic, and hyperchaotic regimes. Additionally, our characterizers provide a detailed, level by level analysis of the short term correlations in the system and analyze the network structure in much greater detail than the usual network characterizers such as average path lengths or clustering coefficients. Our methods, therefore, provide a set of new and powerful tools for the analysis of dynamical systems.

I. INTRODUCTION

The analysis of the time series of the variables of evolving dynamical systems is an important tool for analyzing the dynamical behavior of nonlinear dynamical systems, as well as for making predictions for their behavior. A variety of well developed methods and tools are used to carry out this kind of analysis, which also define a set of precise metrics such as the Fourier transforms, power spectra, generalized dimensions and entropies, multifractal spectra, and Lyapunov exponents.¹

In recent years, traditional techniques for the analysis of time series have been supplemented by new approaches, which draw on areas such as nonlinear time series analysis,² data mining, and complex networks.³ These approaches complement the traditional techniques and provide important additional insights into the behavior of evolving dynamical systems. An important recent method of analyzing time series consists of mapping these time series to networks, which are then called time series (TS) networks. A number of methods are available for carrying out this mapping. These include constructing networks from pseudoperiodic time series,⁴ the use of visibility graphs,⁵ the quantile mapping,⁶ recurrence time networks,^{7–9} etc. These network representations are then analyzed using a variety of well known network metrics such as clustering coefficients, degree distributions, and path lengths.^{10,11}

In this paper, we analyze the time series networks (TS networks) obtained from distinct dynamical regimes of evolving maps and flows, using methods of algebraic topology,^{12–14} and recently constructed measures, which analyze the simplicial structure of graphs.¹⁵ The TS networks are constructed from the time series by using the visibility algorithm,⁵ which has certain advantages over other methods. The graphs so constructed are then analyzed using the simplicial characterizers, which reveal the hierarchical levels of complexity hidden in the TS network, which arise due to the correlations of the original time series.

We show that the methods are able to identify the crucial differences between the time series corresponding to distinct dynamical behaviors. We analyze the networks using the usual network characterizers and demonstrate that the simplicial characterizers, which include both global and local quantities, provide a more sensitive and accurate diagnosis of the dynamical characteristics of the underlying time series. While the conventional network characterizers give us the global structural information of the network, the local dynamical information is embedded in the simplicial complexes and their interconnections at various topological levels. In essence, this formalism uncovers the hidden skeleton of the dynamics of the systems.

We have used multiple metrics that characterize not only the global properties related to the network structure, but also identify the hidden skeleton in the form of hierarchical levels of complexity that expose the underlying dynamics and the short term correlations of the system. We use the logistic map, the Hénon map, the generalized Lozi map, and the Lorenz system as test beds, as their dynamics is well understood and has been characterized using a variety of conventional quantities such as Lyapunov exponents, entropies, etc. We compare the information extracted from our topological characterizers with that obtained from these quantities and identify elements that can be generalized to other cases. We note that the use

of characterizers from algebraic topology is slowly finding acceptance in the analysis of complex systems. These include the use of persistent homologies for the topological characterization and early detection of bifurcations,^{16,17} as well as the analysis of high dimensional data.¹⁸ Our methods can also contribute to the effective analysis of these cases.

This paper is organized as follows. We use the time series data from the systems considered at parameter values that show distinct kinds of dynamical behaviors. To map these time series data sets into their corresponding network representations, we employ the visibility algorithm,⁵ as explained in Sec. II. We define the measures used to analyze the simplicial structures of the resulting graphs and their connection with the topological structure and topological connectivity in Sec. III. The simplicial characterizers and the usual network characterizers for the systems under study (the logistic map, the Hénon map, the generalized Lozi map, and the Lorenz system) are constructed and tabulated in Secs. IV and V. We summarize and conclude in Sec. VII.

II. THE VISIBILITY GRAPH

In this paper, we use the visibility algorithm developed in Ref. 5 to transform the time series obtained from various dynamical systems evolving in different dynamical regimes into a set of networks. Recent developments show that going from the time series representation to the network representation yields additional information of the underlying dynamics.^{6,19} While a number of methods have been developed over recent years to convert a time series into a network,^{4,6,20} we use the visibility algorithm here due to the simplicity of the visibility approach and its computational efficiency. Additionally, a TS network resulting from the visibility algorithm preserves the structure of the time series, viz., a periodic time series gives rise to a regular graph, a random time series gives rise to a random graph, and a fractal time series gives rise to a scale-free graph.⁵ We note that the visibility algorithm has been used in diverse contexts ranging from finance²¹ to geophysics.²²

The visibility algorithm introduced in Ref. 5 is implemented as follows. Given a time series, visibility graphs are constructed by considering time data points as nodes, and a link is established between any two nodes if and only if there is no obstruction in the line of sight of these two nodes. Let the pair of points (y_i, t_i) denotes the data in the time series for $i = 1, 2, \dots, N$. For any two pairs (y_i, t_i) and (y_j, t_j) to be visible to each other (by line of sight visibility), all other intermediate data pairs (y_r, t_r) should satisfy the condition,

$$y_j > y_r + \frac{y_j - y_i}{t_j - t_i} (t_r - t_i) \quad (1)$$

(see Fig. 1 for a graphical representation of the algorithm).

We use the visibility algorithm to construct the TS network graphs for time series obtained from different dynamical regimes of the logistic map and other evolving dynamical systems. Network representations of the time series can be seen in Ref. 19 but have not been further analyzed by quantitative methods. We use the methods of algebraic topology to construct a set of characterizers, which can be used to analyze these TS networks. Since the dynamical systems that contribute to the time series are very well understood, the TS networks studied here constitute good test beds for analyzing the

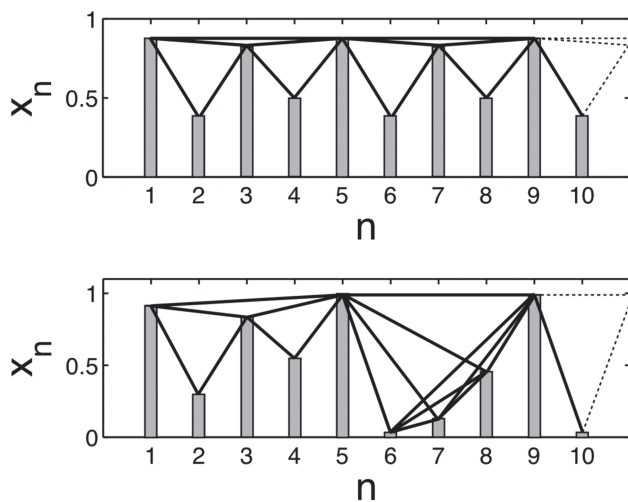


FIG. 1. The visibility algorithm illustrated for period-4 (top panel) and chaotic (bottom panel) time series, obtained from the logistic map at $\mu = 3.5$ and $\mu = 4.0$, respectively, and their visibility connections.

effectiveness of the algebraic topology methods for the analysis of dynamical regimes.

III. THE DEFINITIONS OF THE SIMPLICIAL CHARACTERIZERS

Here, we study the topological structural properties of the networks generated by the visibility algorithm. The connectivity and topological properties of the network graphs reflect the connections between the dynamical states of the system in time.^{14,23} The networks so obtained are further classified using the concepts of *cliques* and *simplices*.^{24,25} We summarize these below.

In our context, a graph or a network represents a collection of interacting nodes interconnected by links or edges. We define a clique to be a maximal complete subgraph; i.e., the nodes of a clique are not part of a larger complete subgraph. Using the adjacency matrix of the network, the Bron-Kerbosch algorithm²⁴ is used to identify the cliques. The cliques are regarded as the simplices of the graph.

A simplex with $q + 1$ nodes or vertices is a q -dimensional simplex. For instance, a 0-simplex is an isolated point, a 1-simplex is two vertices connected by a line segment, a 2-simplex is a triangle of three connected nodes, a 3-simplex is a tetrahedron with 4 connected nodes, and so on. Furthermore, if two simplices have $q + 1$ nodes in common, they share a q -face. A collection of simplices, which are connected to each other—not just the nodes, but their shared faces as well—form a simplicial complex. The dimension of the simplicial complex is defined as the dimension of the largest simplex in the structure. If we can find a sequence of simplices such that each successive pair shares a q -face, then all the simplices in this sequence are said to be q -connected. Simplices, which are q -connected, are also connected at all lower levels.

In our study, we carry out the structural and connectivity analysis of the TS networks obtained from the time series arising

out of different dynamical regimes of maps and flows of different dimensions, using six topological characterizers, both global and local.^{12–14,23} Three of these quantities are well known and defined in most algebraic topology texts,²⁶ and three are new and have been recently defined in the context of social and traffic networks.^{15,23}

The first characterizer is the vector \mathbf{Q} , known as the first structure vector, which is a measure of the connectivity of the clique complex at various levels. The q th component of $\mathbf{Q} = \{Q_0, Q_1, \dots, Q_{q_{\max}}\}$ is the number of q -connected components at the q th level. The next vector quantity, which we denote by \mathbf{f} , is defined to have the number of q -dimensional simplices as its q th component. The third quantity $\mathbf{N}_s = \{n_0, n_1, \dots, n_{q_{\max}}\}$, known as the second structure vector, has the number of simplices of dimension q and higher as its q th component. The fourth quantity is the third structure vector, $\widehat{\mathbf{Q}}$, which is defined in terms of the previously defined structure vectors \mathbf{Q} and \mathbf{N}_s . Its q th component, \widehat{Q}_q , is given by $\left(1 - \frac{Q_q}{n_q}\right)$. A fifth quantity $\dim Q^i$ is a local quantity, which defines the topological dimension of node i of the simplicial complex, given by

$$\dim Q^i = \sum_{q=0}^{q_{\max}} Q_q^i, \quad (2)$$

where q_{\max} is the dimension of the simplicial complex and Q_k^i is the number of distinct simplices of dimension k in which the node i participates.

Finally, the topological entropy S is defined as

$$S_Q(q) = - \frac{\sum_i p_q^i \log p_q^i}{\log N_q}. \quad (3)$$

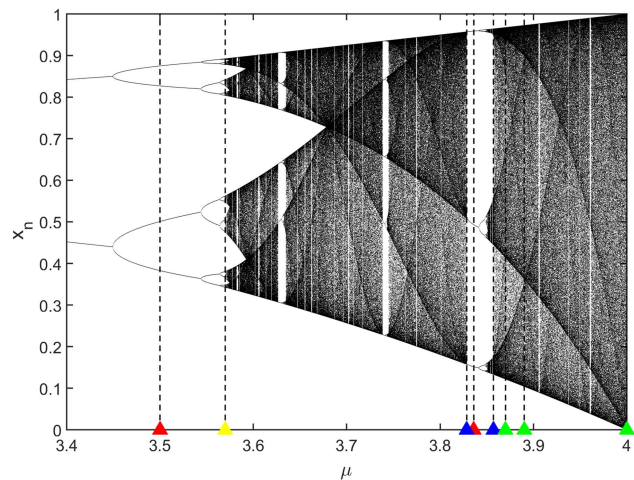


FIG. 2. The bifurcation diagram of the logistic map indicating eight parameter values at which time series are obtained—periodic: $\mu = 3.5$ and $\mu = 3.836$ (red triangles), intermittent: $\mu = 3.8284$ and $\mu = 3.857$ (blue triangles), Feigenbaum point: $\mu = 3.56995$ (yellow triangle), and chaotic: $\mu = 3.87$, $\mu = 3.89$, and $\mu = 3.857$ (green triangles).

TABLE I. Structure vectors \mathbf{Q} , \mathbf{N}_s , and $\hat{\mathbf{Q}}$ for the logistic map TS networks. These TS networks are constructed from a time series of length 2000 (after discarding the first 5000 points) using the visibility algorithm.

	μ q -level	Periodic		Intermittent		Feigenbaum	Chaotic		
		3.5 Period 4	3.836 Period 3	3.8284 Before P3	3.857	3.569 95	3.87 Chaos 1	3.89 Chaos 2	4.0 Full chaos
\mathbf{Q}	0	1	1	1	1	1	1	1	1
	1	501	667	559	139	128	97	84	77
	2	1498	666	842	1115	1871	1384	1386	1117
	3		666	587	695		451	463	459
	4			10	48		56	58	192
	5			1	3		12	10	77
	6							1	38
	7								20
	8								15
	9								4
\mathbf{N}_s	0	1499	667	853	1166	1872	1478	1489	1228
	1	1499	667	853	1166	1872	1478	1489	1228
	2	1498	666	851	1165	1871	1476	1488	1228
	3		666	590	710		474	483	509
	4			10	48		61	62	214
	5			1	3		12	10	92
	6							1	50
	7								25
	8								15
	9								4
$\hat{\mathbf{Q}}$	0	0.9993	0.9985	0.9988	0.9991	0.9995	0.9993	0.9993	0.9992
	1	0.6658	0	0.3447	0.8808	0.9316	0.9344	0.9436	0.9373
	2	0	0	0.0106	0.0429	0	0.0623	0.0685	0.0904
	3		0	0.0051	0.0211		0.0485	0.0414	0.0982
	4			0	0		0.0820	0.0645	0.1028
	5			0	0		0	0	0.1630
	6							0	0.24
	7								0.2
	8								0
	9								0

Here, $p_q^i = Q_q^i / \sum_i Q_q^i$ is the probability of a particular node i participating in a q -simplex, and $N_q = \sum_i (1 - \delta_{Q_q^i, 0})$ denotes the number of nodes that participate in at least one q -simplex.

The TS network graphs are analyzed using these six simplicial characterizers. The calculation is illustrated for a simple example in the [Appendix](#). The simplicial characterizers obtained for the actual TS network graphs obtained from time series taken from the logistic map, Hénon map, generalized Lozi map, and Lorenz system at different parameter values are discussed in Sec. [IV–VI](#).

IV. SIMPLICIAL CHARACTERIZERS FOR THE LOGISTIC MAP

In this section, our objective is to investigate the connection between the topological structure arising out of the TS network and the underlying dynamics of the evolving system, in this case

the logistic map, which is defined by $x_{n+1} = \mu x_n(1 - x_n)$, for the full spectrum of dynamical behavior that it shows, namely, periodic, intermittent, and chaotic.

We are interested in identifying the signature of specific dynamical behaviors of the evolving system in the topological characterizers of the respective networks. The time series of the logistic map has been obtained at eight distinct values of parameters, where distinct classes of dynamical behavior are seen. These parameter values have been indicated in the bifurcation diagram in [Fig. 2](#) and include representative samples, from the periodic, intermittent, and chaotic regimes of the logistic map and also at the edge of chaos. The six simplicial characterizers defined above have been calculated for the TS networks obtained using the time series data for $t = 2000$ time steps, after discarding the initial 5000 transients. Therefore, the TS networks have $N = 2000$ nodes. The visibility condition [given in Eq. (1)] has been implemented with a tolerance of $\epsilon = 10^{-4}$.

TABLE II. The topological response function \tilde{f} and the topological entropy S for the logistic map TS networks. These TS networks are constructed from a time series of length 2000 (after discarding the first 5000 points) using the visibility algorithm.

	μ q -level	Periodic		Intermittent		Feigenbaum	Chaotic		
		3.5 Period 4	3.836 Period 3	3.8284 Before P3	3.857	3.569 95	3.87 Chaos 1	3.89 Chaos 2	4.0 Full chaos
\tilde{f}	0	0	0	0	0	0	0	0	0
	1	1	1	2	1	1	2	1	0
	2	1498	0	261	455	1871	1002	1005	719
	3		666	580	662		413	421	295
	4			9	45		49	52	122
	5			1	3		12	9	42
	6							1	25
	7								10
	8								11
	9								4
S	0	0	0	0	0	0	0	0	0
	1	1	1	0.9464	1	1	1	1	0
	2	0.9774	0	0.9697	0.9752	0.9620	0.9779	0.9765	0.9742
	3		0.9923	0.9919	0.9838		0.9783	0.9766	0.9786
	4			0.9763	0.9806		0.9824	0.9848	0.9869
	5			1	1		0.9707	0.9731	0.9912
	6							1	0.9930
	7								0.9758
	8								0.9938
	9								1

The dynamical regimes are

1. The periodic regime: This was studied at two parameter values, viz., $\mu = 3.5$ (period-4 behavior) and $\mu = 3.836$ (period-3 window).
2. The edge of chaos: $\mu = 3.569\,95$ (Feigenbaum point, period-2 cascade ends here).
3. Intermittency: For this, we studied the values $\mu = 3.8284$ (the onset of crisis induced intermittency) and $\mu = 3.857$ (postcrisis induced intermittency).
4. The chaotic dynamical regimes are $\mu = 3.87$ (chaos), $\mu = 3.89$ (chaos), and $\mu = 4.0$ (fully developed chaos).

As mentioned above, the time series data at these parameter values are transformed to networks using the visibility algorithm, and the clique structure of the resulting network is extracted using the Bron-Kerbosch algorithm.²⁴ Furthermore, the six topological quantities are calculated for these networks. The results of the analysis are presented in Tables I–III. Two central aspects of the network characterizers quantified by the six quantities are topological structure and topological connectivity.

1. The topological connectivity between the simplices at each topology level is identified by the simplicial characterizer \mathbf{Q} . The vector \mathbf{Q} measures the number of connected components (i.e., simplicial complexes) of the network at each topology level—for $q = 0$ (at least one vertex in common), $q = 1$ (at least two vertices in common), $q = 2$ (at least three vertices in common),

etc. To understand this, consider period 4 ($\mu = 3.5$), for which $Q = [1, 501, 1498]$. Here, Q_0 counts the number of components that are 0-connected. For the period-4 example, $Q_0 = 1$, which means that all simplices in the network have at least one node in common with each other. From Table I, we observe that for all the μ values considered, at the lowest topology level ($q = 0$), the components of \mathbf{Q} have a value of 1, confirming that there is no isolated node in the network, in any of the dynamical regimes.

Second, the second element Q_1 counts the number of components made up of simplices that have at least two nodes in common; i.e., components that are 1-connected. We see from

TABLE III. The maximum value of the topological dimension of all nodes in the TS network of the logistic map at the parameter values indicated in the table. The time series considered is of length 2000.

μ	Nature of orbit	$\max(\dim Q^i)$
3.5	Period 4	4
3.836	Period 3	2
3.569 95	Feigenbaum point	8
3.828 4	Intermittency before P3	8
3.857	Intermittency	12
3.87	Chaos 1	13
3.89	Chaos 2	13
4	Full chaos	12

Table I that for period-4, $Q_1 = 501$, i.e., there are 501 simplicial complexes that are individually made up of simplices that have at least two nodes in common. In other words, there are 501 1-connected components for the period-4 trajectory.

Next, the third element Q_2 counts the number of components made up of simplices that have at least 3 nodes in common, i.e., that are 2-connected. For period-4, $Q_2 = 1498$. This means that there are 1498 components that are made up of simplices that have 3 nodes in common with each other. Note that in this case, $q_{\max} = 2$, which means that the highest dimension of simplex in the structure is 2. This implies that the largest simplex in the structure is a triangle. So, $Q_2 = 1498$ simply counts the number of disconnected triangles in the network. We note that all the periodic regimes, including the Feigenbaum point, have contributions to the components of Q only up to $q = 2$ or $q = 3$, indicating that in all the periodic regimes of the logistic map, the largest simplicial structure is a triangle or a tetrahedron, and the connections range from 3-connections to 0-connections. The more complex dynamical regimes, viz., the intermittent and chaotic regimes, have more complex structures. The intermittent regimes (see Table I) have tetrahedral, pentahedral, and hexahedral structures and connections up to the 5-connection level. The chaotic regime has simplicial structures all the way up to the 10-dimensional simplex level and connections up to the 9-connection levels. This has been verified for both the 2000 and 10 000 point time series, with the visibility condition implemented to a tolerance of $\epsilon = 10^{-4}$.

We also compare the simplicial characterizer Q for the intermittent value ($\mu = 3.8284$) and the chaotic values $\mu = 3.87$ and 3.89 in Table I. The number of simplices at the chaotic value increases much more sharply at the $q = 2$ level, before they decrease, as compared to the intermittent case where the number of connected components at each level changes much more gradually. We note that at $\mu = 3.87$, we see contributions up to the $q = 5$ level and the $q = 6$ level for $\mu = 3.89$, whereas at $\mu = 4.0$, where fully developed chaos is seen, the contributions continue to the $q = 9$ level (see Table I).

- The second structure vector N_s is a running index, which counts the number of connected components at level q and above; i.e., it is a cumulative index for \tilde{f} . It, therefore, contains the same information as seen in \tilde{f} at the $q = 9$ level, for the chaotic regimes. Again, the periodic and chaotic regimes show completely distinct behavior, with contributions for the periodic regime and the Feigenbaum point, being confined to the first three q -levels, whereas the $\mu = 4$ case sees contributions up to the $q = 9$ level. The intermittent case ($\mu = 3.8284$) and the value $\mu = 3.89$ in the chaotic regime again reflect the difference seen in the case of the first structure vector.
- The components of the third structure vector, \hat{Q} , are defined in terms of the extent to which the ratio $\frac{Q_q}{n_q}$ differs from 1. This quantity thus lies between zero and one. Here again, there is a sharp difference between the periodic and chaotic cases and the intermittency at $\mu = 3.8284$ and the chaotic value $\mu = 3.87$ and $\mu = 3.89$.
- The vector \tilde{f} quantifies most directly the topological structure of the network. This vector counts the number of simplices at

each topological level and functions like a response function. As noted earlier, we see that the periodic regimes show behavior quite distinct from the chaotic regimes. In the periodic regimes, the response function \tilde{f} increases sharply with level so that most of the simplices are at the topmost level, whereas in the chaotic regimes, the response function peaks sharply at the third level ($q = 2$) and then decreases gradually so that the plot has a long tail, extending up to $q = 9$.

The differences between the intermittent value at $\mu = 3.8284$ and the chaotic values $\mu = 3.87$ and 3.89 also show up clearly in Table II. We see a clear shift in the level at which the highest value of the number of simplices occurs. There are some contributions now at the $q = 6$ and $q = 7$ levels for these cases, as compared to the $\mu = 4.0$ case, which has contributions until the $q = 9$ levels. Thus, the case of fully developed chaos is clearly differentiated from the others, by its long tail, as seen for the Q vector above. These features can also be seen in Fig. 3.

- The topological entropy $S(q)$ is a measure of the complexity of the network as well. This is shown in Table II. The entropies of the periodic states and the edge of chaos contribute up to the $q = 2$ levels, whereas the fully developed chaos state shows contributions until the $q = 9$ level. The intermittent cases and the chaotic cases show small fluctuations relative to each other at the different levels, with contributions up to the $q = 6$ and 7 levels.
- The quantity $\max(\dim)Q^i$ gives the maximum value of the topological dimension of all the nodes in the network. (Refer to Table III for the 2000 node TS network.) This picks the changes in the dynamic regimes most strongly.

We see a clear distinction between the periodic states and the intermittent and chaotic states in this case. For the periodic states, the node in the network, which participates in the most number of simplices, participates in a very few simplices, the values being 4 and 2, for the period 3 and period 4 values. At the edge of chaos, viz., $\mu = 3.56995$, there is at least one node that participates in 8 simplices.²⁷ A higher value, viz., 13, is seen in the intermittent regime.²⁸ At $\mu = 4.0$, viz., fully developed chaos, there is a node that participates in as many as 12 simplices.²⁹ Thus, there are many more interconnections in the chaotic regimes compared to the periodic ones.

The values of the topological characterizers in Tables I–III are for a 2000 node network obtained out of a time series evolving from a single initial condition. The same qualitative features are observed for simplicial characterizers for longer time series of 10 000 points. This can be further supported by examining the behavior of the normalized quantities. If we plot the normalized Q and \tilde{f} values as functions of the q -level for time series of lengths 500, 2000, and 10 000 points, we see that these plots not only follow the same trends, but also collapse on top of each other. For the periodic regime, the collapse is perfect, as is expected. In the case of the intermittent and chaotic regimes, the value of q_{\max} increases with the length of the time series, as is also expected, but the same qualitative behavior is seen (see Fig. 3).

A. $\max(\dim)Q^i$ and the Lyapunov exponent

The $\max(\dim)Q^i$, i.e., the dimension of the node that participates in the largest number of simplices of any dimension, is a

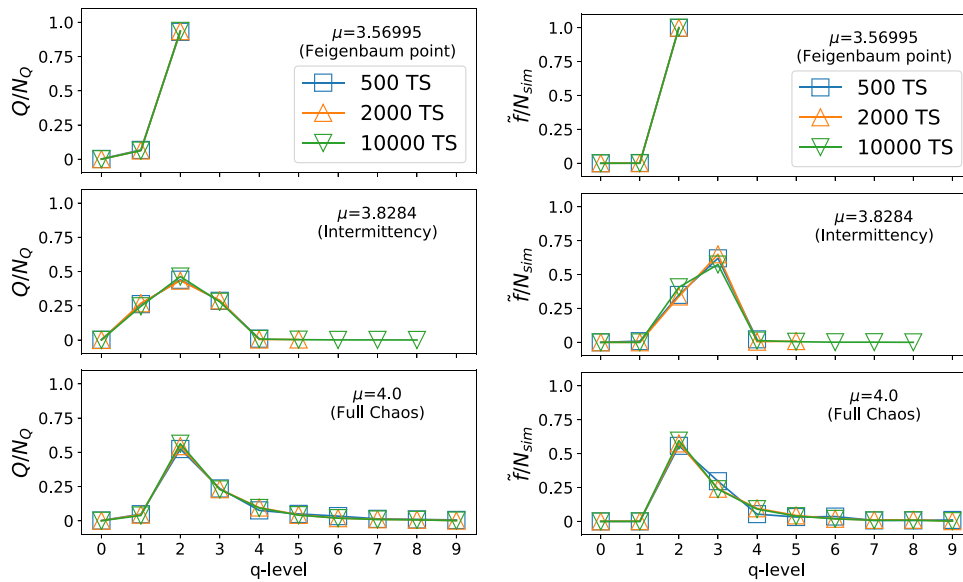


FIG. 3. Plots of the normalized simplicial characterizers \mathbf{Q} (left panel) and \tilde{t} (right panel) for the logistic map, for the Feigenbaum point ($\mu = 3.56995$), intermittency ($\mu = 3.8284$), and full chaos ($\mu = 4$) cases, for TS networks of 500 (blue square), 2000 (orange downward triangle), and 10 000 (green upward triangle) sizes. Here, $N_0 = \sum_q Q_q$ and $N_{sim} = \sum_q \tilde{t}_q$.

measure of the complexity of the correlations in the time series at that value of the parameter μ . It is interesting to compare its behavior with the Lyapunov exponent, which is a measure of the chaoticity, as encoded by the rate of divergence of two neighboring trajectories at the given value of the parameter. Figure 4 plots the $\max(\dim) Q^i$ as a function of the parameter μ for the parameter range $3.5 \leq \mu \leq 4.0$, as well as the Lyapunov exponent vs μ for the same range. Here, we plot the average value of $\max(\dim) Q^i$ for 20 distinct initial conditions at each μ value (in black), along with the standard deviation, in gray.

It is instructive to compare the behavior of the $\max(\dim) Q^i$ with that of the Lyapunov exponent in different parameter regimes. In the period doubling regime, we first note that the $\max(\dim) Q^i$ is a constant across the window of each period and jumps at each period doubling bifurcation, indicating the change in the network connectivity that reflects each period. It is also the same for all the initial conditions, in the stable regime of the period. Since the TS network corresponding to each period repeats its characteristic pattern, the $\max(\dim) Q^i$ is also characteristic of each period and shows increasing values with increasing period. In contrast, the Lyapunov exponent in the periodic regime shows negative values, which decrease with the increase in the stability of the period, with the exponent value decreasing to $-\infty$ at the location of the superstable orbit. As the period becomes unstable, the Lyapunov exponent value touches zero. Thus, the Lyapunov exponent and the $\max(\dim) Q^i$ contain complementary information. The $\max(\dim) Q^i$ contains information about the structure of the periodic trajectory and the Lyapunov exponent about its stability. Again, both quantities are useful for detecting the bifurcation boundary at the edge of its period.

These properties of the $\max(\dim) Q^i$ can be observed for the entire period doubling cascade, which accumulates at the Feigenbaum point at $\mu = 3.56995 \dots$. Beyond this point, the fact that the trajectories have now crossed into the chaotic regime is reflected by a jump to a higher value of $\max(\dim) Q^i$. The value of $\max(\dim) Q^i$

is now much more sensitive to initial conditions, as is expected in the chaotic regime, and the average value, therefore, fluctuates much more as a function of parameter μ . The existence of periodic windows in the chaotic regime is signaled by a corresponding drop in the values of $\max(\dim) Q^i$, at the appropriate values of μ . We note that the average value of $\max(\dim) Q^i$ fluctuates in a narrow band in the entire chaotic regime, similar to the behavior of the Lyapunov exponent. The increased sensitivity to initial conditions is also seen at the point of intermittency, indicating the presence of strong fluctuations.

We note that while the Lyapunov exponent is a time averaged quantity, the $\max(\dim) Q^i$ is, in contrast, a local measure. As mentioned above, the $\max(\dim) Q^i$ can be used as a complementary quantity in addition to the global measures to gain insights on the dynamical nature and transitions that arise in the analysis of time series. So far, we discussed the results of the six topological characterizers that were used to analyze the time series networks for various dynamical regimes of the logistic map. We shall now subject these dynamical regimes to a more standard analysis using the conventional complex network characterizers in Sec. IV B.

B. Using conventional network characterizers

In this section, we employ three of the widely used conventional complex network characterizers, viz., the average clustering coefficient c and the characteristic path length l ,^{10,30} to carry out the standard analysis of the network properties of the TS networks obtained from the logistic map time series for different dynamical regimes. We use the same time series data as used for the simplicial characterization, viz., the logistic map time series for 2000 time steps after discarding 5000 initial transients and the resultant TS network of 2000 nodes. The standard network characterizers are defined in Secs. IV B 1–IV B 3. We first examine these characterizers separately and then examine them together.

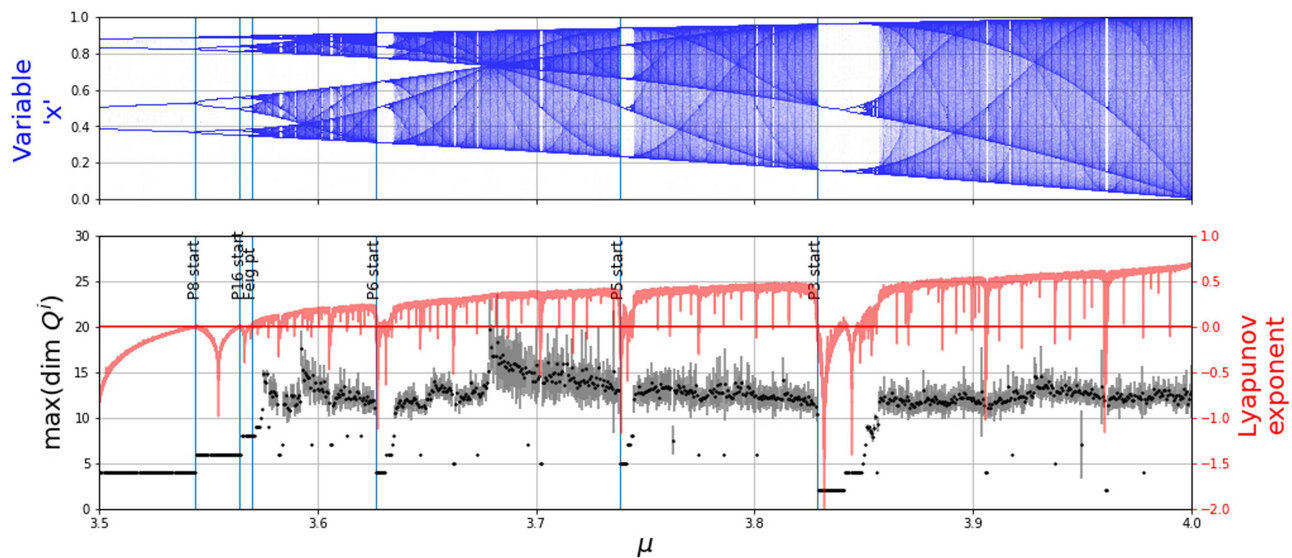


FIG. 4. The average maximum topological dimension $\max(\dim Q')$ (in black) for logistic map TS networks as a function of parameter μ (averaged over 20 initial conditions) and its standard deviation (in gray), along with the Lyapunov exponent (in red). The bifurcation diagram is replicated on top for easy reference.

1. Clustering coefficient

First, the average clustering coefficient c of a network measures the extent to which a network is interconnected, i.e., to what extent are the neighbors of a given node neighbors of each other. If a node i is connected to k other nodes, then the clustering coefficient c_i of the node i is defined as the ratio of the actual number of connections that exist between the k nodes to the maximum number of interconnections that can exist between the k nodes. If the actual number of interconnections that exist between k nodes that are linked to the node i is given by E_i , then the maximum number of interconnections possible between the k nodes is simply C_2^k , which is $k(k-1)/2$. Thus, the clustering coefficient of node i is defined as $c_i = 2E_i/k(k-1)$.

We first examine the clustering coefficient c for TS networks of different dynamic regimes. In Table IV, the second column lists the clustering coefficient spanning over the entire range of values of μ . We see that these values of c that correspond to different dynamical regimes—periodic, intermittent, and chaotic dynamics—all fall in a narrow range, $0.6913 < c < 0.7858$. Each period has a network characteristic of its own period. The clustering coefficients for different periods, however, differ by very small values. For high periods, the tolerance to which the visibility condition is evaluated also plays a role. The values for intermittent and chaotic regimes do not fall within distinct ranges. Thus, the clustering coefficient c is neither able to distinguish between distinct dynamic regimes nor is able to club together similar regimes.

2. Characteristic path length

The second characterizer that we look at is the average path length l of the TS network (see Table IV), i.e., the average distance between arbitrarily chosen points. Here, the average path length l takes larger values in periodic regimes (i.e., at $\mu = 3.5$ and 3.836) and

at the edge of chaos (Feigenbaum point, $\mu = 3.56995$) than that at the μ values corresponding to intermittency ($\mu = 3.8284$ and 3.857). Small values of the average path lengths are seen at the chaotic values $\mu = 3.87$ and $\mu = 3.89$ and at the fully developed chaos value $\mu = 4.0$. The reason for the existence of large path lengths in the periodic regime is clear. The periodic networks have simplices that connect among near neighbors, and many short steps are necessary to connect points, which are far apart on the time series. In terms of the simplicial analysis above, the network structures corresponding to periodic orbits have a significantly large number of regular simplices that are connected at lower topological levels. For instance, for $\mu = 3.5$ and $\mu = 3.836$, the first structure factor Q has a large component at the $q = 1$ level, $Q_1 = 501$ and $Q_1 = 667$, respectively.

TABLE IV. The conventional characterizers—the clustering coefficient (c) and the average path length (L)—for parameters of the logistic map corresponding to various dynamical regimes. In generating the TS network, we discarded 5000 initial transients and used 2000 time steps in the time series; as a result, the TS network has nodes $N = 2000$. Calculations of these characterizers were made using NetworkX, a Python language package for network analysis.

μ	c	L	λ	Nature of orbit
3.5	0.6913	167.9995	−0.8725	Period 4
3.836	0.7998	222.9999	−0.2306	Period 3
3.569 95	0.6932	44.2464	0.0050	Feigenbaum point
3.828 4	0.7811	193.5178	0.1109	Intermittency before P3
3.857	0.7760	46.4710	0.2766	Intermittency
3.87	0.7317	34.0742	0.4265	Chaos 1
3.89	0.7320	29.1327	0.4982	Chaos 2
4	0.7858	27.4089	0.6931	Full chaos

This means that the resultant network is sparsely interconnected, and its average path length is large.

On the other hand, for the intermittent and chaotic cases, the corresponding TS networks contain links that connect points, which are widely separated on the network. These long range links imply that widely separated nodes can be reached in far fewer steps, leading to short average path lengths. In the simplicial language, the chaotic TS networks have a large number of regular simplices, which are rather sparsely connected at a lower topological level ($q = 1$ and $q = 2$) but are better connected at a higher topological level ($q = 2$ and higher). The resulting network, therefore, is an overall better interconnected network giving rise to a significantly low average path length.

It is interesting to speculate whether there are any regimes, which have a small world connectivity, e.g., at the Feigenbaum point or the edge of chaos. However, the present data do not permit any definite conclusion. This question will be examined elsewhere.

3. Degree distributions

The cumulative degree distributions of the TS networks obtained at the μ values of interest are plotted in Fig. 5. It is clear that the periodic networks have many nodes whose interconnections follow identical patterns, and hence, there are only a finite number of degrees. This can be seen for $\mu = 3.450$ (period 4) and $\mu = 3.828\,43$, the onset of period 3. The degree distribution starts showing a bigger variation, over one decade, at the onset of chaos ($\mu = 3.569\,95$). This expands further at $\mu = 3.857\,00$, at the onset of crisis induced intermittency, and even more so at the chaotic value $\mu = 3.880\,00$ and $\mu = 4.0$, i.e., at fully developed chaos. The log-log plots of these distributions show short regimes where a power-law can be fitted. However, even the 10 000 node networks do not really show scale-free behavior.

We note that unlike the usual characterizers, our simplicial description is capable of identifying network motifs and is in fact more general than what is provided by network motifs, since it can identify the ways in which the network motifs are put together, the regularity with which they occur, and also motifs at different levels of topological complexity. We hope to discuss this in more detail in future work.

V. SIMPLICIAL CHARACTERIZERS FOR HIGHER DIMENSIONAL SYSTEMS

We have thus seen that the simplicial characterizers are able to capture the distinct behavior seen in different dynamical regimes of the logistic map and are able to capture the contribution of the correlations in the system. This is particularly important in the chaotic regime where the correlations are short term, and their contribution is difficult to characterize using the usual characterizers. We have also carried out a detailed comparison of the simplicial characterizer $\max(\dim)Q^i$ with the Lyapunov exponent. Similar analysis can be carried out for any other 1-dimensional system and will yield a similar distinction between dynamical regimes.

It is now interesting to see if the simplicial characterizers can distinguish between the dynamical regimes of high dimensional systems, maps as well as flows. For this, we study two maps, the Hénon

map (2-dimensional), and the generalized Lozi map (3-dimensional), as well as the Lorenz flow. Here, the 2-dimensional Hénon map possesses both periodic and chaotic regimes, and the 2-dimensional and 3-dimensional Lozi maps demonstrate chaotic and hyperchaotic behavior. We note that the simplicial characterizers carry distinct signatures of these dynamical behaviors. We undertake a similar exercise in the Lorenz system to demonstrate that the simplicial characterizers can distinguish between periodic and chaotic dynamical cases.

A. Hénon map

We first consider the Hénon map³¹ defined by the equations

$$\begin{aligned}x_{n+1} &= 1 - ax_n^2 + y_n, \\ y_{n+1} &= bx_n.\end{aligned}\quad (4)$$

We consider the dynamics of this system for two parameter sets, for the values $a = 1.05$; $b = 0.3$, where the system displays periodic behavior with a period-8 orbit, and for $a = 1.4$; $b = 0.3$, where the system displays chaotic behavior. We have calculated the full set of simplicial characterizers for both these cases.

As might be expected, the periodic case shows a very simple structure. For the period-8 case, all the characterizers only contribute up to the $q = 2$ level (see Fig. 7). Most prominently, the $\tilde{\mathbf{f}}$ -vector, which counts the number of simplices at each level, only has contributions at the $q = 2$ level (triangles), for the period-8 case.

In contrast, the chaotic case shows that all the characterizers contain contributions up to the $q = 5$ level indicating far more complex structures. Here, the $\tilde{\mathbf{f}}$ -vector has contributions up to the $q = 5$ level for the chaotic case, indicating the presence of simplices, which are triangles, tetrahedrons, and pentagons. These reflect the hierarchy of short term correlations in the system (see Fig. 8). We note that the number of connected components peaks at the $q = 2$ level, in both cases, but a substantial number of more complicated structures are seen in the chaotic case. This is reflected in the second and third structure vectors as well as the entropy S .

The final characterizer, the $\max(\dim)Q^i$, assigns a compact numerical value to the complexity. We saw that in the case of the logistic map, $\max(\dim)Q^i$ plotted as a function of the map parameter μ proved to be an effective characterizer of dynamical regimes, similar to the plot of the conventional Lyapunov exponent vs μ . Here, for the Hénon map, we plot the value of $\max(\dim)Q^i$ for $b = 0.3$ for values of a ranging from 1.0 to 1.3 in Fig. 6. The Lyapunov exponent for the same set of parameters is plotted on the same graph, and the bifurcation diagram of the system for the variable x is also plotted in Fig. 6 in the top panel. We observe again that the $\max(\dim)Q^i$ picks up the same set of features here, as it does for the logistic map, viz., $\max(\dim)Q^i$ is a constant across the window of each period and jumps at each period doubling bifurcation, with a value that is characteristic of each period, and is stable to initial conditions in the periodic regime. In the chaotic regime, $\max(\dim)Q^i$ jumps to higher values, indicating the increase in the complexity of correlations, and is much more sensitive to initial conditions, leading to larger fluctuations in the average value. Like the Lyapunov exponent, it also picks up successfully the periodic windows in the chaotic regime, as in the logistic map case, via a corresponding drop

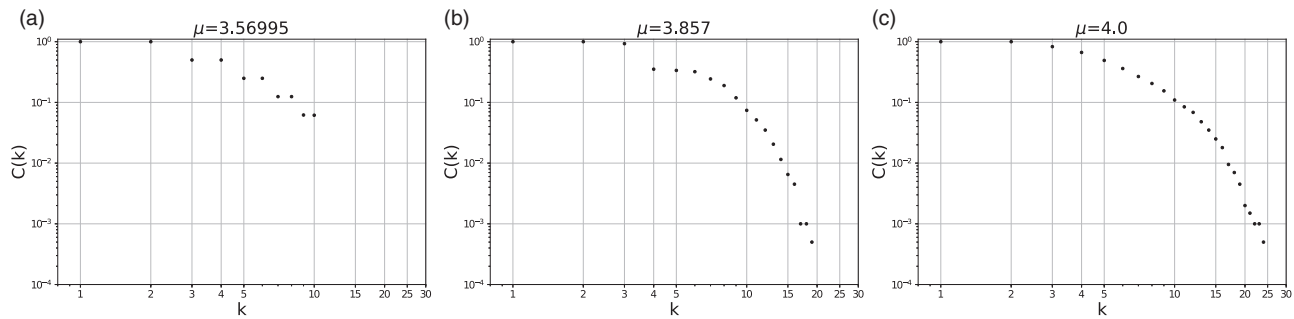


FIG. 5. Cumulative degree distributions for logistic map TS networks at (a) $\mu = 3.56995$ (Feigenbaum point), (b) $\mu = 3.857$ (intermittency), and (c) $\mu = 4.0$ (full chaos). Length of TS = 2000.

in its value at the appropriate values of the parameter a . We note here that the period doubling bifurcations, as well as the periodic windows in the chaotic regimes are picked up as accurately by the $\max(\dim)Q^i$ as by the Lyapunov exponent. Here, again, it remains complementary to the Lyapunov exponent, as it picks up the structure of the period over the entire stability interval, whereas the Lyapunov exponent quantifies the stability of the period over the stability interval.

We note that in this as well as all subsequent cases, the time series considered is of length 2000 after discarding the transients of length 5000, unless otherwise stated. The network constructed here is constructed out of the time series for the x variable, using the visibility algorithm. The network constructed using the y variable gives similar results. Section V B discusses the comparison between chaos and hyperchaos using the generalized Lozi map.

B. The generalized Lozi map

To see the differences between chaotic and hyperchaotic behavior, we examine the generalized d -dimensional Lozi map³² defined by the equations,

$$\begin{aligned} x_{n+1}^1 &= 1 - a|x_n^k| + (1 - \nu)x_n^d, \\ x_{n+1}^2 &= x_n^1, \\ &\vdots \\ x_{n+1}^d &= x_n^{d-1}, \end{aligned} \quad (5)$$

where the superscript represents the variable index and the subscript represents the time index, with the constraint $k < d$ from the definition. This is a piecewise linear map, and parameters a and ν

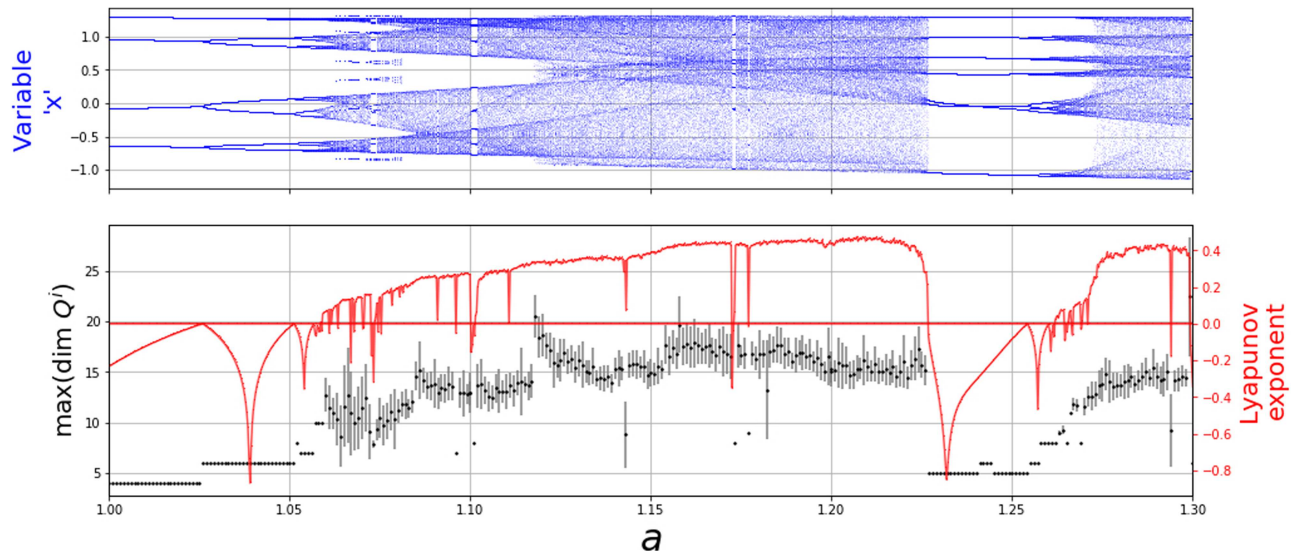


FIG. 6. The average maximum topological dimension $\max(\dim) Q^i$ (in black) for Hénon map TS networks as a function of the parameter a (averaged over 20 initial conditions) and its standard deviation (in gray), along with the Lyapunov exponent (in red) and the bifurcation diagram (in blue).

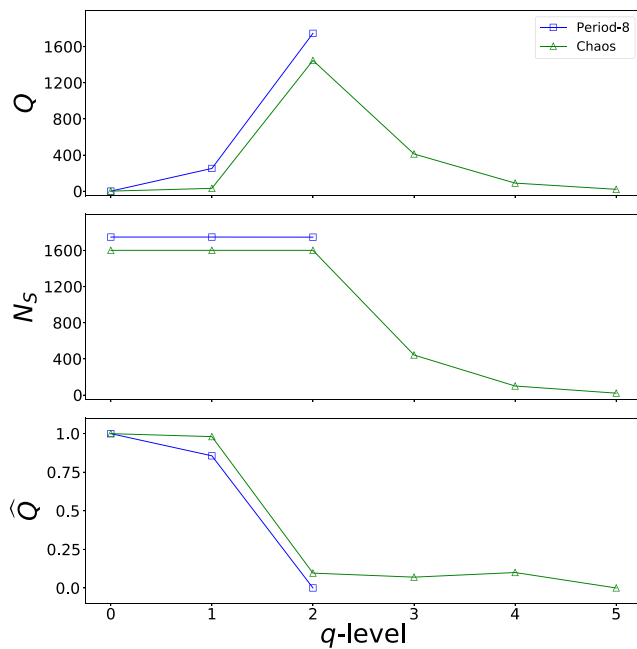


FIG. 7. Plots of the simplicial characterizers Q , N_s , and \hat{Q} for the Hénon map for the period-8 case, i.e., at the parameter values $a = 1.05$ and $b = 0.3$ (blue) and for the chaotic case at the values $a = 1.4$ and $b = 0.3$ (green).

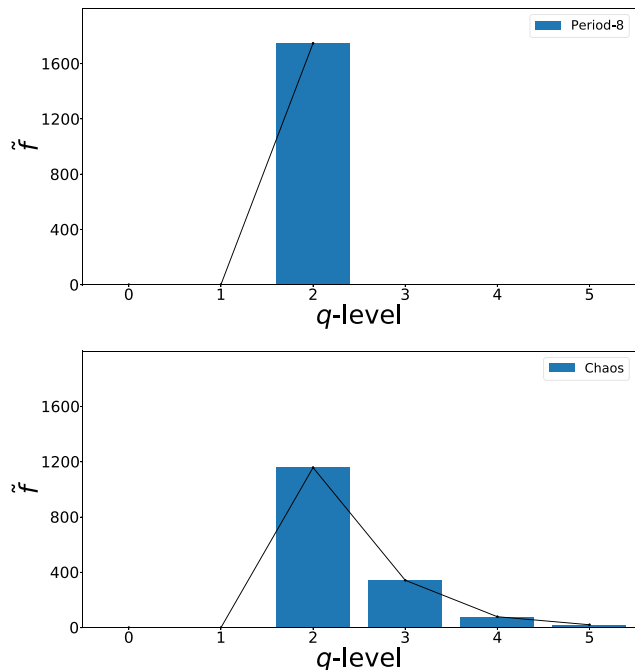


FIG. 8. Plots of the simplicial characterizers \tilde{f} for the Hénon map for the period-8 case, i.e., at the parameter values $a = 1.05$, $b = 0.3$ (blue), and for the chaotic case at the values $a = 1.4$, $b = 0.3$ (green).

control, respectively, the nonlinearity and dissipation of the system. We focus on the three-dimensional Lozi map (with $d = 3$, $k = 2$) that displays hyperchaotic dynamical behavior at certain parameter values. The dynamical equations for this map are as follows:

$$\begin{aligned} x_{n+1}^1 &= 1 - a|x_n^2| + (1 - \nu)x_n^3, \\ x_{n+1}^2 &= x_n^1, \\ x_{n+1}^3 &= x_n^2. \end{aligned} \quad (6)$$

Chaotic behavior is seen at parameter values $(a, \nu) = (0.75, 1.75)$, and at the values $(a, \nu) = (1.3, 0.6)$, we see hyperchaos.

There are very distinct differences between the simplicial characterizers of the chaotic and hyperchaotic cases. The number of simplices at level q , i.e., the \tilde{f} -vector peaks at $q = 2$ for the chaotic case, whereas it peaks at $q = 3$ for the hyperchaotic case (see Fig. 9). Thus, the dominant simplices are triangles in the chaotic case (as in the case of the chaotic Lozi map) and tetrahedra in the hyperchaotic case. The Q -vector, which counts the number of connected components at the q th level, also contains significant information. The chaotic case shows a sharp increase in Q at the $q = 2$ level (1070 2-connected simplicial complexes) so that most connections between simplices in the chaotic case are links, whereas in the hyperchaotic case, they are at $q = 3$ (1012 3-connected simplicial complexes); i.e., most connections between simplices are 2-faces or triangles. In both cases, there are significant contributions at the 2, 3, and 4 levels. How-

ever, there are nonzero contributions up to level $q = 6$ for the chaotic case and $q = 7$ for the hyperchaotic case, contributing to a long tail as in the earlier examples.

As before, the most direct indication of complex correlations comes from the quantity the $\max(\dim)Q^i$ (see Table V). We see that the $\max(\dim)Q^i$ is significantly higher in the hyperchaotic case (23.0 ± 2.5) compared to the chaotic case (14.65 ± 1.63). Here, an average is taken over 20 initial conditions. The highest and lowest values observed for the $\max(\dim)Q^i$ for this set of initial conditions are 13 and 18 for the chaotic case and 17 and 27 for the hyperchaotic case.

We also carry out a comparison of the standard network characterizers for the TS networks obtained for the periodic (Hénon), chaotic (Hénon, generalized Lozi), and the hyperchaotic cases (generalized Lozi) in Table V. As in the logistic map case, the clustering coefficient does not clearly differentiate between the dynamical regimes; however, the path lengths shorten with increase in the complexity of the network. Thus, long path lengths are seen for the periodic case (Hénon) and short path lengths are seen for the chaotic and hyperchaotic cases, with the shortest path lengths being seen for the hyperchaotic case.

Our next case is that of a flow, viz., the Lorenz system.

TABLE V. Standard network characterizers, Lyapunov exponents, and $\max(\dim)Q^i$ for the Hénon map and generalized Lozi map.

Parameters	Dynamical regime	c	L	Lyapunov exponents	$\max(\dim)Q^i$
<i>Hénon map</i>					
$a = 1.05$, $b = 0.3$	Period-8	0.6931 ± 0.0001	85.2483 ± 0.0007	$(-0.0125, -1.191)$	6 ± 0
$a = 1.4$, $b = 0.3$	Chaos	0.733 ± 0.002	13.7 ± 1.6	$(0.416, -1.620)$	14.95 ± 0.89
<i>Generalized Lozi map</i>					
$a = 0.75$, $v = 1.75$	Chaos	0.732 ± 0.001	9.90 ± 1.10	$(0.069, -0.160, -0.197)$	14.65 ± 1.63
$a = 1.3$, $v = 0.6$	Hyperchaos	0.748 ± 0.001	6.92 ± 0.47	$(0.142, 0.123, -1.181)$	23.0 ± 2.5

C. Lorenz system

The evolution equations for the well known Lorenz system are

$$\begin{aligned}\dot{x} &= \sigma(y - x), \\ \dot{y} &= x(\rho - z) - y, \\ \dot{z} &= xy - \beta z,\end{aligned}\quad (7)$$

where σ , ρ , and β are parameters of the system.

We study the Lorenz system at two sets of parameter values, $\sigma = 10$, $b = 8/3$, and $r = 160$ where periodic behavior is seen and

$\sigma = 10$, $b = 8/3$, and $r = 60$ where chaotic behavior is seen. This time series is sampled at a delay time³³ for which the mutual information entropy has its first minimum.³⁴ The x -variable of this flow is plotted in Fig. 10, where the time series of the Lorenz system with a step size of $\delta t = 0.005$ (using the Runge-Kutta algorithm) and a sampling interval obtained from the delay time technique $\Delta t = 0.165$. It can be seen from Fig. 10 that the variations of the time series are captured accurately by this sampling time.

The visibility graph of the system is constructed using this time series, which yields a dense and closely packed visibility graph for the chaotic case. The graphs for both the periodic and chaotic cases are analyzed using our simplicial characterizers. As earlier, more complex correlations and graphs are expected for the chaotic case. The vector $\tilde{\mathbf{f}}$ for the periodic case ($\sigma = 10$, $b = 8/3$, and $r = 160$) peaks at level $q = 2$ (951 triangular simplices) and falls off rapidly up to $q = 5$ (28 simplices). In contrast, the $\tilde{\mathbf{f}}$ for the chaotic case ($\sigma = 10$, $b = 8/3$, and $r = 60$) peaks at a higher level $q = 3$ (455 tetrahedral simplices), has large contributions at the $q = 4$ level

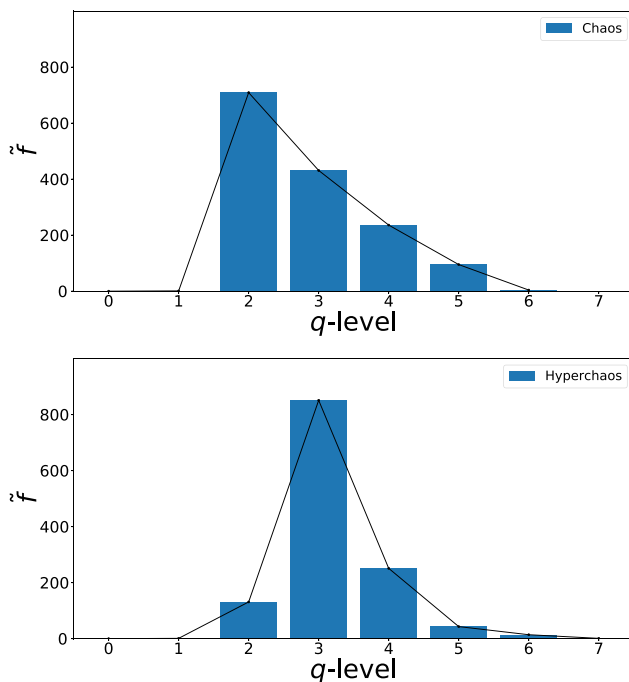


FIG. 9. Simplicial characterizer plots for the generalized Lozi map for a chaotic orbit, i.e., $a = 0.75$, $v = 1.75$ (blue), and a hyperchaotic orbit, i.e., $a = 1.3$, $v = 0.6$ (green).

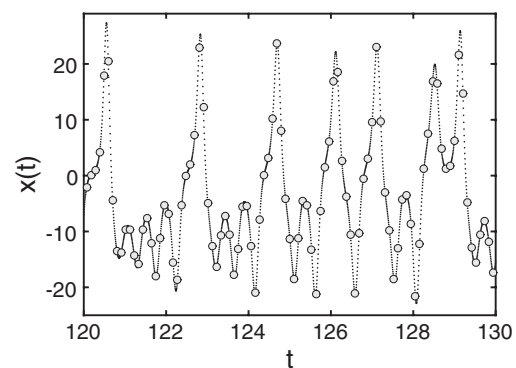


FIG. 10. The coarse grained time series (symbols) used for the visibility algorithm from the Lorenz time series (small dots) for the x variable. For the coarse graining time interval, we adapt the time delay obtained from the first minimum of the mutual information.³⁴ Thus, the coarse graining intervals are $\tau_x = 21\delta t$, with $\delta t = 0.005$ s being interval size of the original time series. The resulting coarse grained data (spanned by the symbols in the plot) are used to construct the visibility graphs in order to extract the essential dynamical features of the system.

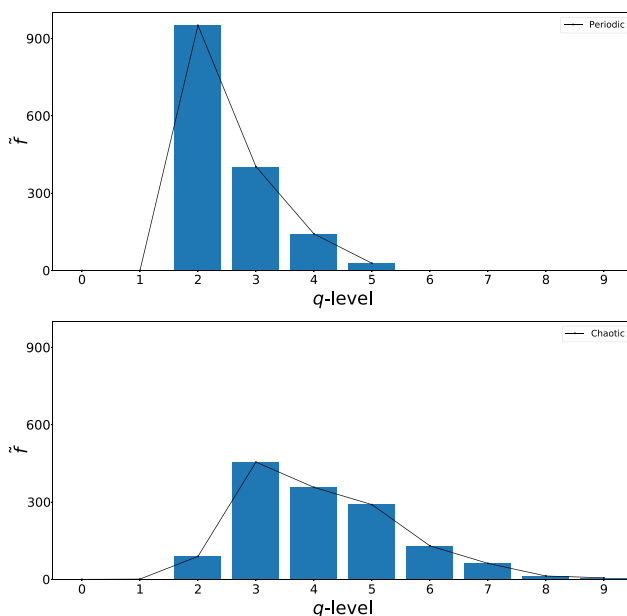


FIG. 11. Plots of the simplicial characterizer \tilde{r} for the Lorenz system for the periodic case, i.e., at the parameter values $\sigma = 10$, $\beta = 8/3$, $\rho = 160$ (top), and for the chaotic case at the values $\sigma = 10$, $\beta = 8/3$, $\rho = 60$ (bottom).

(357 pentagonal simplices) and $q = 5$ level (290 hexagonal simplices) as well, and has nonzero contributions up to $q = 9$ (130 6-simplices, 62 7-simplices, and 6 9-simplices). This can be seen in Fig. 11. This can be understood from the way in which the periodic and chaotic trajectories are supported by the two-lobed butterfly attractor and the structure of the corresponding graphs. The signature of higher complexity can be seen for the other simplicial characterizers as well. For the periodic case, the \mathbf{Q} vector has a peak at the $q = 2$ level and contributions up to $q = 5$. In contrast, for the chaotic case, the \mathbf{Q} shows its first peak at $q = 3$ with $Q_3 = 667$ and falls off gradually until the level $q = 9$. This is reflected in the $\max(\dim)Q^i$ values as well. For the periodic case seen at $r = 160$, $\max(\dim)Q^i = 12$, and for the chaotic case at the value $r = 60$, $\max(\dim)Q^i = 30$, which is well differentiated and much higher than all the periodic cases. Thus, the simplicial characterizers for the Lorenz flows show the same trends as are seen in the high dimensional maps.

VI. COMMENTS ON COMPUTATIONAL ISSUES

We note that the details of the TS networks show some sensitivity to the accuracy of computation. For example, the visibility condition is evaluated to some tolerance ϵ . This condition makes a difference to the details of the network in some cases, particularly in the case of the Feigenbaum attractor, and leads to small changes in the values of the topological characterizers, especially the exact value of $\max(\dim)Q^i$. Similarly, different initial conditions also lead to slightly different values of the topological characterizers, and therefore, averages over initial conditions lead naturally to noninteger values of the topological characterizers. We note, however, that the

changes are small, and the qualitative behavior of the topological quantities as functions of the level q maintains the behavior that is shown in the graphs, with each kind of behavior being characteristic of the given dynamical regime.

The visibility graphs constructed here have been constructed using the x variable time series, including the high dimensional cases, viz., the Hénon map, generalized Lozi map, and Lorenz flow. We note for the maps considered here, the other variables are scaled versions of the x variable. Hence, the visibility graphs, which are invariant under affine transformation of the series data,⁵ remain the same if the time series variable is changed, and therefore, the simplicial characterizers remain the same.

In the case of the Lorenz flow, we have used the x -variable, sampled at a delay time that corresponds to the minimum of the mutual information entropy,³ to construct the time series graph, since by Taken's embedding theorem, the time delayed versions of one generic variable are sufficient to embed the n -dimensional manifold. We hope to explore the issue of embedding as well as other modes of constructing networks in future work.

VII. CONCLUSION

To summarize, we examine the TS networks obtained from the time series of the logistic map, Hénon map, generalized Lozi map, and Lorenz system using algebraic topology methods. Our characterizers are clearly able to distinguish between chaotic and periodic regimes. Furthermore, these characterizers can also distinguish between chaotic and hyperchaotic regimes. The simplicial structure of time series networks associated with all these dynamical regimes contains nodes, links, and triangular faces and also contains fully connected clique complexes. The periodic regimes are characterized by regular graphs, which contain simplices of smaller dimensions, compared to the simplices in the chaotic time series networks.

While the dynamical stability of dynamical systems is well understood, and quantified nicely by the Lyapunov exponent, the short term correlations of evolving systems, especially in the chaotic regime, have not been quantified to any great extent. The TS networks constructed by the visibility method encode these correlations in terms of the connectivity of the network graphs. The simplicial characterizers uncover the hidden geometry of these graphs, level by simplicial level, by providing a precise quantification of the manner in which these graphs are connected, pointwise, linkwise, triangle-wise, and higher. This is very clear from our tables, as well as from the graphs. This is analogous to the manner in which the multifractal structure analyzes the scaling behavior of a multiscale set. To the best of our knowledge, there is no analysis of the short term correlations in an evolving system that does this, including entropic analysis. The algebraic characterizers and their identification of the hierarchy of geometrical structures can also contribute to the identification of dominant network motifs in general complex networks.

We also note that our local topological quantity, viz., the maximum dimension that counts the number of simplices in which the most highly connected node participates, is highly sensitive to the dynamic nature of time series and quantifies the strong increase in the connectivity properties of the network seen at the edge of chaos, in the chaotic regime, and the hyperchaotic regime, very accurately. In the context of the logistic map and Hénon map, the maximum

dimension plotted as a function of the map parameter μ provides detailed insight into the changes in dynamical behavior and complements the information available in the Lyapunov exponent. The utility of the algebraic topological quantifiers is thus demonstrated in simple contexts where the dynamical behavior is well understood.

A comparison with the usual network characterizers is also necessary here. The clustering coefficient is much the same for all the examples, in all the dynamic regimes. This indicates that the clique formation in the distinct dynamic regimes is not significantly different. However, the short path lengths on the network in the chaotic and hyperchaotic regimes studied encode the fact that the connections formed here are long range connections on the network, as opposed to the long path lengths (and short range connections) in the periodic regime. It is interesting to note that for the logistic map, the edge of chaos (the Feigenbaum point) and the chaotic regime at the end of the period 3 window show path length values, which are clearly separated from both these regimes. This small-world-like behavior is in line with other observations, which indicate distinctly different behavior at the edge of chaos. This point deserves further investigation and needs to be supplemented by further investigation of the simplicial structure at the edge of chaos. A detailed comparison of the level by level correlations in chaotic and hyperchaotic regimes is also a further direction of study.

Thus, the algebraic topological characterizers of time series networks appear to be promising candidates for revealing the hidden geometry of networks, which represent time series with nontrivial correlations between dynamical states. We expect them to be particularly useful in situations, which exhibit phase transitions or other significant changes in the dynamics, such as jamming behavior and unstable dimension variability. We note that our description is capable of identifying network motifs and is in fact more general than what is provided by network motifs, since it can identify the ways in which the network motifs are put together, the regularity with which they occur, and also motifs at different levels of topological complexity. We hope our study will motivate future work in these directions.

ACKNOWLEDGMENTS

N.G. and N.N.T. thank the CSIR scheme [No. 03(1294)/13/EMR-II] for partial support.

APPENDIX: CALCULATION OF SIX CHARACTERIZERS USING A SIMPLE EXAMPLE

Let us take the simplicial complex in Fig. 12 where two triangular simplices are connected by a link. The simplicial complex here has three simplices, the third one being the simplex made of two nodes with a single link between them. We shall now use this simplicial complex to illustrate how the six characterizers are calculated.

The three simplices of the simplicial complex are denoted by $A = \{1, 2, 3\}$, $B = \{2, 4\}$, and $C = \{4, 5, 6\}$, with the vertices labeled as shown in Fig. 12. The incidence matrix Λ of the simplicial complex can be written as a matrix with the simplex index as rows and the node index as columns. If a node is contained in a simplex, then the corresponding element in the matrix is 1 or else it is 0. We, therefore,

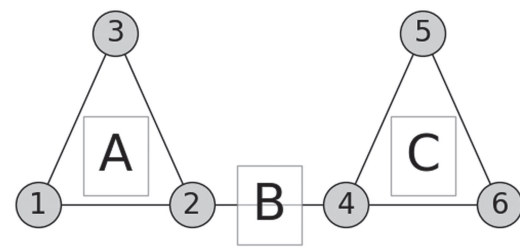


FIG. 12. An illustration to demonstrate connectivity between three simplices in a simplicial complex. Two simplices A and C are of dimension $q = 2$, and the third simplex B is of dimension $q = 1$. Simplices A and C are 0-connected to simplex B , which means that each of them has a single vertex in common with B . We use this example to illustrate the calculation of all the six characterizers in the Appendix.

have

$$\Lambda = \begin{pmatrix} 1 & 1 & 1 & 0 & 0 & 0 \\ 0 & 1 & 0 & 1 & 0 & 0 \\ 0 & 0 & 0 & 1 & 1 & 1 \end{pmatrix}.$$

Both the simplices A and C are of dimension 2, as they have 3 nodes each, and the simplex B has a dimension 1, because it has 2 nodes. Note that if a simplex has $q + 1$ nodes, then it is of dimension q .

Let us first calculate the first structure vector \mathbf{Q} for the simplicial complex.

1. First structure vector \mathbf{Q}

Let us consider the first structure vector \mathbf{Q} for the simplicial complex. Since the simplices A and B are with three nodes (their dimension being 2), the structure vector \mathbf{Q} will have three levels: $q = 0$, $q = 1$, and $q = 2$. If two simplices are to be q -connected, they should have at least $q + 1$ nodes in common, and also that if two simplices are q -connected, then they are also connected at all lower topological levels.

In our example, at the $q = 0$ level, for topological connectivity between any two simplices, we need at least one node in common. By this, we see both the pairs A and B as well as B and C are connected, as they have one common node each, node-2 and node-4, respectively. In fact, the whole simplicial complex made up of three simplices A , B , and C is now identified as one entity at the $q = 0$ topological level.

At the next level $q = 1$, for connectivity between two simplices, we need at least two nodes to be in common. As we have none, all the three simplices are disconnected from each other at this level. The total number of entities is now three.

At the $q = 2$ level, none of the simplices are connected for it requires a minimum of three nodes to be in common. In addition, at the $q = 2$ level, only the simplices A and B with dimension 3 exist. Therefore, we see only two entities at this level. In all, the first structure vector is $\mathbf{Q} = (1, 3, 2)$.

2. Second structure vector \mathbf{N}_s

The second structure vector \mathbf{N}_s is defined as follows. The q th component of \mathbf{N}_s is the number of simplices present in the simplicial complex at level q and higher. At the level $q = 0$, we can see

from Fig. 12 that the total number of simplices here is three, $n_0 = 3$. Next, at level $q = 1$, the number of simplices is again three, $n_1 = 3$, and at level $q = 2$, the number is two, $n_2 = 2$. Therefore, the second structure vector is $\mathbf{N}_s = (3, 3, 2)$.

3. Third structure vector $\hat{\mathbf{Q}}$

The q th component of the third structure vector $\hat{\mathbf{Q}}$ is given by $1 - Q_q/n_q$, where Q_q and n_q are the q th components of the first and second structure vectors, respectively. Therefore, we can get $\hat{\mathbf{Q}} = (2/3, 0, 0)$.

4. $\tilde{\mathbf{f}}$ vector

Here, the q th component is the number of simplices at level- q . At level $q = 0$, we have to count the number of simplices that are isolated nodes. Our simplicial complex does not have any isolated nodes; thus, $\tilde{f}_0 = 0$. Therefore, at level $q = 0$, there are no simplices that have one isolated node; as a result, $\tilde{f}_0 = 0$.

At the next level $q = 1$, the only simplex to have two nodes is the simplex B ; thus, $\tilde{f}_1 = 2$. For level $q = 2$, two simplices A and C have three nodes each, and we have $\tilde{f}_2 = 2$. We can now write the vector as $\tilde{\mathbf{f}} = (0, 1, 2)$.

5. Maximum topological dimension: $\max(\dim) \mathbf{Q}^i$

To find the maximum topological dimension of the simplicial complex, we need to find the topological dimension Q^i of all the nodes. The topological dimension of a node i is the number of simplices of dimension- q (the same as level- q) the node participates in. For node-1, it takes part only in the simplex A , which is at level-2. Therefore, the only nonzero component of the vector \mathbf{Q}^1 is for level-2, $\mathbf{Q}^1 = (0, 0, 1)$. Similarly, node-2 participates in two simplices A , of dimension 2, and B , of dimension-1. Therefore, the vector \mathbf{Q}^1 will have nonzero contributions for levels-1 and 2, giving $\mathbf{Q}^2 = (0, 1, 1)$.

Working out in a similar fashion, we will have the vectors for the four other nodes in the simplicial complex as follows. $\mathbf{Q}^3 = (0, 0, 1)$, $\mathbf{Q}^4 = (0, 1, 1)$, $\mathbf{Q}^5 = (0, 0, 1)$, and $\mathbf{Q}^6 = (0, 0, 1)$.

The topological dimensions that a node participates are then the sum of the nonzero components of that node (row sum of the vector \mathbf{Q}^i). We, therefore, have $Q^1 = 1$, $Q^2 = 2$, $Q^3 = 1$, $Q^4 = 2$, $Q^5 = 1$, $Q^6 = 1$, among which the maximum dimensionality is seen in nodes Q^2 and Q^4 with a value 2, which is the value of $\max(\dim) \mathbf{Q}^i$.

6. Entropy S

The entropy of a topological level- q is defined by

$$S(q) = \frac{-\sum_i p_q^i \log p_q^i}{\log N_q},$$

where p_q^i is the occupation probability of a node at the level- q , given by $Q_q^i / \sum_j Q_q^j$. The quantity $N_q = \sum_i (1 - \delta_{Q_q^i, 0})$ is the number of nodes that have a nonzero entry at the level- q in the simplicial complex. The delta function in N_q will take the value of unity if the subscript $Q_q^i = 0$ or else it will be zero.

Now, the occupation probability p_i is obtained from the topological dimensions Q_q^i (calculated above). At level $q = 0$, Q_q^i is zero for all

the nodes; as a result, $p_i = 0$ and entropy $S_Q(0) = 0$. At level $q = 1$, only nodes 2 and 4 contribute to the topological dimension. That is, $Q_1^2 = 1$ and $Q_1^4 = 1$; all else are zero. The corresponding occupation probabilities are $p_1^2 = 1/2$ and $p_1^4 = 1/2$. The entropy at level $q = 1$ is $S(1) = 1$.

Finally, at level $q = 2$, all the nodes contribute to the topological dimension, $Q_2^i = 1$, which gives a value of $p_2^i = 1/6$. Then, the entropy at the level $q = 2$ is $S(2) = 1$.

The quantities defined here can now be computed for the actual TS networks in a similar way.

REFERENCES

- H. Kantz and T. Schreiber, *Nonlinear Time Series Analysis*, 2nd ed. (Cambridge University Press, 2004).
- H. D. Abarbanel, *Analysis of Observed Chaotic Data* (Springer-Verlag, New York, 1996).
- Z.-K. Gao, M. Small, and J. Kurths, "Complex network analysis of time series," *Europhys. Lett.* **116**, 50001 (2017).
- J. Zhang and M. Small, "Complex network from pseudoperiodic time series: Topology versus dynamics," *Phys. Rev. Lett.* **96**, 238701 (2006).
- L. Lacasa, B. Luque, F. Ballesteros, J. Luque, and J. C. Nuño, "From time series to complex networks: The visibility graph," *Proc. Natl. Acad. Sci. U.S.A.* **105**, 4972–4975 (2008).
- A. S. L. O. Campanharo, M. I. Siler, R. D. Malmgren, F. M. Ramos, and L. A. N. Amaral, "Duality between time series and networks," *PLoS One* **6**, e23378 (2011).
- N. Marwan, J. F. Donges, Y. Zou, R. V. Donner, and J. Kurths, "Complex network approach for recurrence analysis of time series," *Phys. Lett. A* **373**, 4246–4254 (2009).
- L. Trulla, A. Giuliani, J. Zbilut, and C. Webber, "Recurrence quantification analysis of the logistic equation with transients," *Phys. Lett. A* **223**, 255–260 (1996).
- M. V. Caballero-Pintado, M. Matilla-García, and M. Ruiz Marín, "Symbolic recurrence plots to analyze dynamical systems," *Chaos* **28**, 063112 (2018).
- D. J. Watts and S. H. Strogatz, "Collective dynamics of 'small-world' networks," *Nature* **393**, 440–442 (1998).
- R. Albert and A.-L. Barabási, "Statistical mechanics of complex networks," *Rev. Mod. Phys.* **74**, 47–97 (2002).
- R. H. Atkin, "From cohomology in physics to q-connectivity in social science," *Int. J. Man. Mach. Stud.* **4**, 139–167 (1972).
- L. Duckstein and S. A. Nobe, "Q-analysis for modeling and decision making," *Eur. J. Oper. Res.* **103**, 411–425 (1997).
- X. H. Kramer and R. C. Laubenbacher, "Combinatorial homotopy of simplicial complexes and complex information systems," in *Applications of Computational Algebraic Geometry: American Mathematical Society short course, January 6–7, 1997, San Diego, California* (American Mathematical Society, 1998), pp. 91–118.
- M. Andjelković, N. Gupte, and B. Tadić, "Hidden geometry of traffic jamming," *Phys. Rev. E* **91**, 052817 (2015).
- K. Mittal and S. Gupta, "Topological characterization and early detection of bifurcations and chaos in complex systems using persistent homology," *Chaos* **27**, 051102 (2017).
- S. Maletić, Y. Zhao, and M. Rajković, "Persistent topological features of dynamical systems," *Chaos* **26**, 053105 (2016).
- C. Giusti, R. Ghrist, and D. S. Bassett, "Two's company, three (or more) is a simplex," *J. Comput. Neurosci.* **41**, 1–14 (2016).
- B. Luque, L. Lacasa, F. J. Ballesteros, and A. Robledo, "Feigenbaum graphs: A complex network perspective of chaos," *PLoS One* **6**, e22411 (2011).
- Y. Yang and H. Yang, "Complex network-based time series analysis," *Physica A* **387**, 1381–1386 (2008).
- Y. Yang, J. Wang, H. Yang, and J. Mang, "Visibility graph approach to exchange rate series," *Physica A* **388**, 4431–4437 (2009).

- ²²J. B. Elsner, T. H. Jagger, and E. A. Fogarty, “Visibility network of United States hurricanes,” *Geophys. Res. Lett.* **36**, L16702, <https://doi.org/10.1029/2009GL039129> (2009).
- ²³S. Maletić and M. Rajković, “Combinatorial Laplacian and entropy of simplicial complexes associated with complex networks,” *Eur. Phys. J. Spec. Top.* **212**, 77–97 (2012).
- ²⁴C. Bron and J. Kerbosch, “Algorithm 457: Finding all cliques of an undirected graph,” *Commun. ACM* **16**, 575–577 (1973).
- ²⁵M. Andjelković, B. Tadić, S. Maletić, and M. Rajković, “Hierarchical sequencing of online social graphs,” *Physica A* **436**, 582–595 (2015).
- ²⁶J. Jonsson, *Simplicial Complexes of Graphs* (Springer-Verlag, Berlin, 2008).
- ²⁷The value of $\max(\dim)Q^i$ at the parameter value corresponding to the Feigenbaum point is higher than that in the periodic regime but lower than that at chaotic points.
- ²⁸Locally, a node in the intermittent regime, which corresponds to a chaotic burst, can be visible to many points in the laminar region, leading to a high value of $\max(\dim)Q^i$.
- ²⁹In addition to $\max(\dim)Q^i$, the signature of higher complexity in the chaotic regime can be seen in the quantity Q as well as q_{\max} , as mentioned earlier.
- ³⁰A.-L. Barabási and R. Albert, “Emergence of scaling in random networks,” *Science* **286**, 509–512 (1999).
- ³¹M. Hénon, “A two-dimensional mapping with a strange attractor,” *Commun. Math. Phys.* **50**, 69–77 (1976).
- ³²S. Bilal and R. Ramaswamy, private communication (2019).
- ³³T. Sauer, J. A. Yorke, and M. Casdagli, “Embedology,” *J. Stat. Phys.* **65**, 579–616 (1991).
- ³⁴A. M. Fraser and H. L. Swinney, “Independent coordinates for strange attractors from mutual information,” *Phys. Rev. A* **33**, 1134–1140 (1986).